



ARTICLE

Enhanced Thermal Performance of Roofing Materials by Integrating Phase Change Materials to Reduce Energy Consumption in Buildings

Chanita Mano and Atthakorn Thongtha*

Department of Physics, Faculty of Science, Naresuan University, Phitsanulok, 65000, Thailand

*Corresponding Author: Atthakorn Thongtha. Email: atthakornt@nu.ac.th

Received: 29 July 2020 Accepted: 24 September 2020

ABSTRACT

This work focused on characterizing and improving the thermal behavior of metal sheet roofing. To decrease the heat transfer from the roof into a building, we investigated the efficiency of four types of phase change materials, with different melting points: PCM I, PCM II, PCM III and PCM IV, when used in conjunction with a sheet metal roof. The exterior metal roofing surface temperature was held constant at 50°C, 60°C, 70°C and 80°C, using a thermal source (halogen lights) for 360 min to investigate and compare the thermal performance of the metal sheet roofing with and without phase change materials for each condition. The thermal behaviors of the phase change materials were analyzed by differential scanning calorimeter (DSC). The results showed the melting points of PCM I, PCM II, PCM III and PCM IV were around 45°C, 50°C, 55°C and 59°C, respectively. The integration of PCM IV into the metal roofing sheet increased the thermal performance by reducing the room temperature up to 2.8%, 1.4%, 1.0% and 0.7% when compared with the normal metal roof sheet, at the controlled temperatures of 50°C, 60°C, 70°C and 80°C, respectively. The thermal absorption of the phase change materials also caused a time delay in the model room reaching a steady temperature. The integration of phase change materials with metal roofing sheets resulted in better thermal performance and conservation of electrical energy by reducing the demand for cooling.

KEYWORDS

Roof; metal sheets; phase change materials; energy saving; thermal storage; building materials

1 Introduction

The energy demand has risen extensively due to the rapid growth of urbanization and population growth [1,2]. There has been an increased awareness of environmental issues, such as a shortage of energy resources and an increase in greenhouse gas emissions [3,4]. The building sector contributes approximately 36% of total energy consumption worldwide, and up to approximately 40% of the energy consumed in buildings was from the cooling load of air conditioners [5,6]. Therefore, enhancing the thermal properties of the building's envelope is an approach to decrease heat transfer into buildings, which can reduce energy consumption by the cooling load, and accordingly reduce greenhouse gas emissions [7,8]. Surprisingly, the heat transferred from building's roof was estimated to be 2.8 times bigger than the heat transferred from the southern facing wall surface (the wall with the maximum amount of solar heat accumulation, the second largest source of heat transfer) [9]. Most of the roofs used on buildings in tropical areas are



constructed using metal roofing sheets, which are not efficient thermal barriers. Roof surface temperatures of over 80°C, have been observed when the afternoon sunlight irradiates the roof [10]. Higher room temperature leads to an increase in energy consumption from air conditioning in buildings.

To reduce heat accumulation and the cooling load of buildings, the integration of phase change materials (PCMs) into building envelope materials is an efficient technique to store thermal energy at high temperatures [11], reduce the thermal transfer through the building envelope and can conserve energy consumption in buildings [12]. PCMs are widely used and based on storing or releasing heat energy during the solid-liquid phase transition to provide useful heating or cooling to keep a relatively constant temperature [13–15]. Alqallaf et al. [16] investigated the thermal performance of a building with a concrete roof fitted with vertical cylindrical holes containing PCM. During the working hours from 12.00 am. to 5.00 pm., the roof containing PCMs could reduce the heat flux to the indoor surface by approximately 12.1% to 17.3% when compared to the concrete roof without PCMs. Alawadhi et al. [17] enhanced the thermal performance of a building's roof by using PCMs as thermal storage. A concrete roof with PCM-filled vertical conical holes was investigated to decrease the heat gain in buildings by around 39% when compared with the same roof without PCM. Meng et al. [18] reduced the heat gain into a building by integrating a PCM layer and a high reflective film into a building's roof, which demonstrated a lower inner surface roof temperature and heat flux reduced by approximately 2.2°C and 66.8% with comparing to a common roof. Košny et al. [19] applied PCM as a heat sink with a photovoltaic (PV) roof to reduce the cooling load of a building during summers. This resulted in a cooling load that was lower than the normal PV roof by up to 50%. Chou et al. [20] designed a sheet metal roof structure with improved total thermal resistance by using a PCM, which improved thermal performance of the new design when compare with the normal roof structure.

In Thailand, the ambient air temperature is in the range of 24–40°C and the mean annual wind speed is in the range of 2.0 m/s [21]. The highest levels of solar radiation are experienced in the months of April and May, measured between 20 and 24 MJ/m²-day and the daily average solar radiation in a full year is around 18.2 MJ/m²-day [22]. These conditions result in significant thermal energy transfer through the roof and results in higher interior temperatures of buildings. To improve the thermal performance of sheet metal roofing, phase change materials were integrated into the sheet metal to decrease the heat transfer through the outer roof surface to the interior areas of the building, resulting in achieving the energy saving goals of buildings. This work was thus focused on examining increasing the thermal performance further of sheet metal roofing, by using phase change materials with various melting points, to achieve energy conservation in buildings.

2 Materials and Methods

2.1 Application and Analysis of the Behavior of Phase Change Materials

Four different types of paraffin were tested as Phase Change Materials (PCMs) to investigate the thermal behavior using a differential scanning calorimeter (DSC). Each type of PCM was formed into a uniform volume of 7 cm × 10 cm × 0.1 cm and was prepared and encapsulated in a polyethylene (PE) container with a thickness of 0.007 mm as shown in Fig. 1. Each PCM unit was arranged and set in a metal wire mesh to fix it in place over a uniform area of 100 cm × 130 cm as shown in Fig. 2. The metal wire mesh was then integrated below the roof to test its thermal performance as illustrated in Fig. 3.

2.2 Model Design and Temperature Measurements under Controlled Temperature

The thermal behavior of the roof was investigated using the PCMs with different melting points under a controlled temperature. Our testing model was built from wood on five sides where each side had an area of 1 m² area and was 5 mm thick and insulated with polyethylene sheets. The ceiling was constructed from gypsum board with thickness of 1 cm to prevent and reduce heat propagation from the roof to the

interior. The roofing in each condition was sheet metal. The sheet metal roofing used had a total thickness (Total Coated Thickness) of 0.025 cm, a curve height of 2.4 cm, a yield strength of approximately 550 MPa, and a density of 2.53 kg/m². The minimum pitch requirement for this roofing material is 12° [23]. Our inclination angle for the roof was approximately 40°.

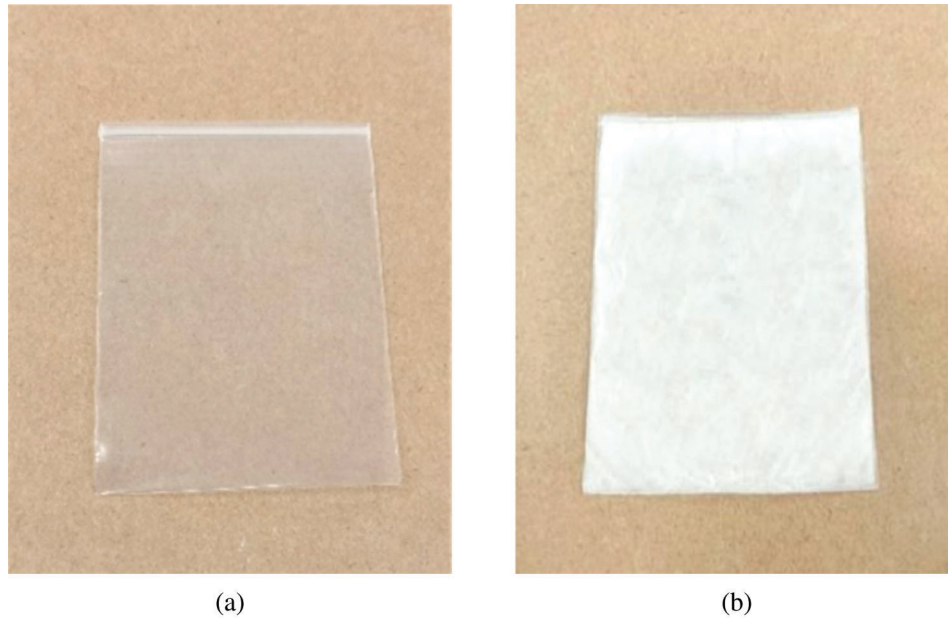


Figure 1: PCM encapsulation. (a) Polyethylene bag, and (b) PCM encapsulated in the polyethylene bag

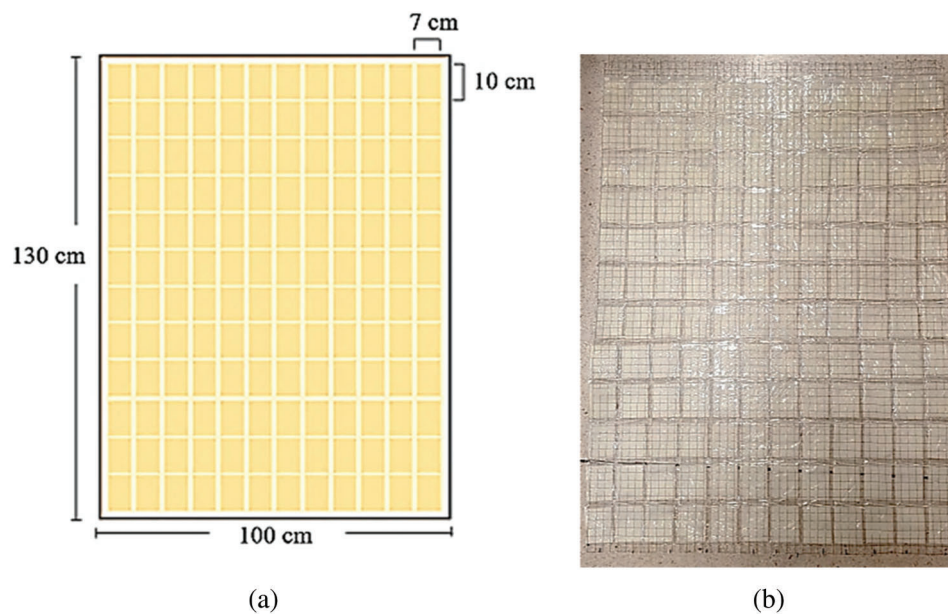


Figure 2: The PCM layout. (a) Dimensions of the PCM layer used for testing, (b) Picture of the PCM layer samples for integrating into the sheet metal roof

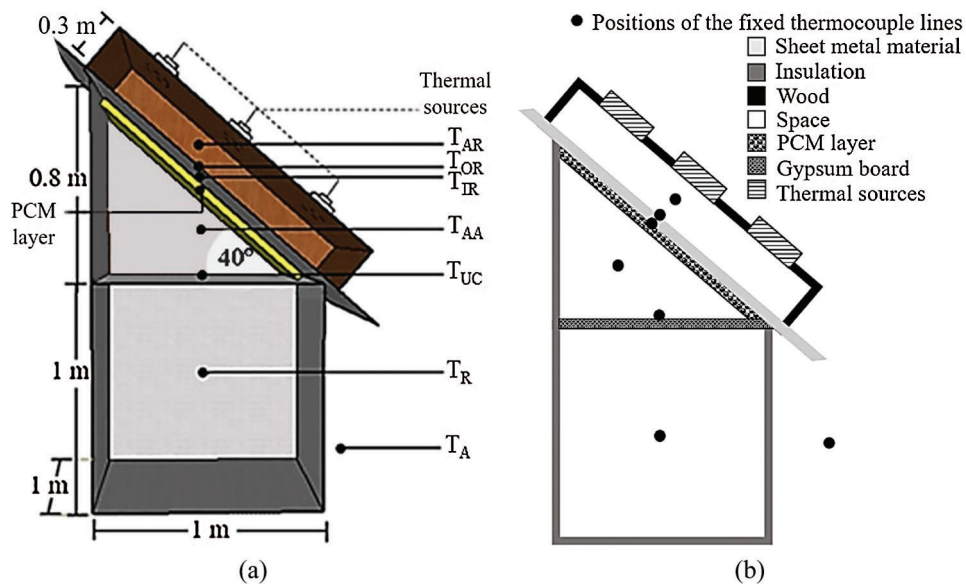


Figure 3: The model for testing. (a) Schematic diagram of the experimental set up, and (b) Positions of the fixed thermocouples to measure the temperature in each condition

Each type of PCM had a uniform area of $100 \text{ cm} \times 130 \text{ cm}$ and was placed in close contact underneath the metal sheet roof. Roofing integrating PCM I, PCM II, PCM III and PCM IV, which have different melting points, were exchanged to test their thermal properties. A thermal source of nine 500 W halogen lamps, placed 0.3 m away from the exterior roof surface, was set up to control the exterior metal roof surface temperature (T_{OR}) at the different temperatures of 50°C , 60°C , 70°C or 80°C for 360 min using a basic voltage control device. The area above the metal roofing sheet (AR), the outside (OR) and inside (IR) the metal roofing sheet surface, inner space area of the attic (AA), upper ceiling surface (UC), center of the interior room (R) and ambient space (A) had the temperature measured with K-type thermocouples with an accuracy of $\pm 0.5^\circ\text{C}$, as illustrated in Fig. 3. The thermocouples installed in the middle of the roof, both inside and outside, and upper ceiling surface, were held in close contact with a thermal aluminum paste to ensure good thermal contact. The ambient temperature was controlled at 27°C by an air conditioner. The temperature at each location was measured in 5 min intervals and recorded continuously for 360 min using a data logger.

3 Results and Discussions

3.1 Thermal Behavior of Phase Change Materials

The thermal behavior of paraffin as a phase change material was analyzed by DSC, from 0°C to 80°C , as shown in Figs. 4–7. The DSC results show the endothermic process curve of the four types of paraffin with different melting points of PCM I, PCM II, PCM III and PCM IV. For PCM I, three endothermic peaks appeared in the range of 0°C and 52°C , as shown in Fig. 4(a). To examine the first peak in more detail, a close up image of the first endothermic peak is shown in Fig. 4(b). The first endothermic peak was found at approximately 15.3°C with a latent heat of 31.20 J/g , which relates to the beginning of paraffin phase transition to a liquid state. A second small endothermic peak was observed around 27.7°C with a latent heat of 6.17 J/g . The last broad endothermic peak was at a temperature around 45.2°C with an involved enthalpy of 67.40 J/g . The second and last endothermic peaks corresponded to the paraffin phase transition from a solid into liquid, and all the peaks are somewhat continuous with the first endothermic peak.

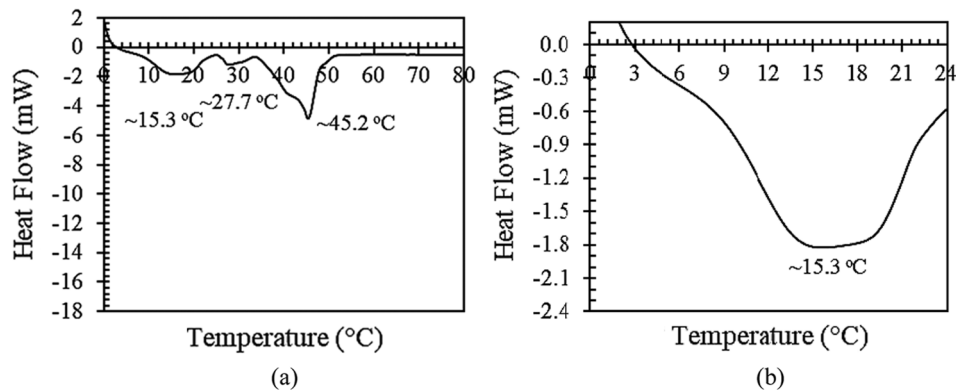


Figure 4: Differential scanning calorimeter plots of PCM I. (a) The endothermic process curve in the temperature range of 0°C to 80°C and (b) Zoomed in on the first endothermic peak

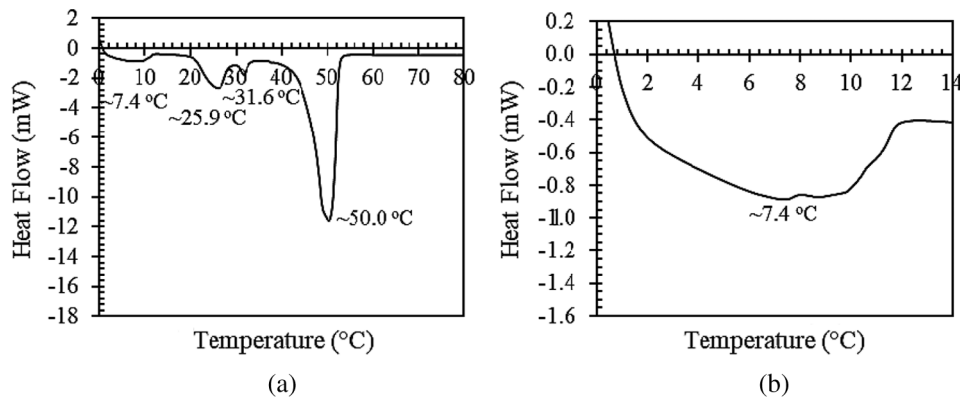


Figure 5: Differential scanning calorimeter plots of PCM II. (a) The endothermic process curve in the temperature range of 0°C to 80°C, and (b) Zoomed in on the first endothermic peak

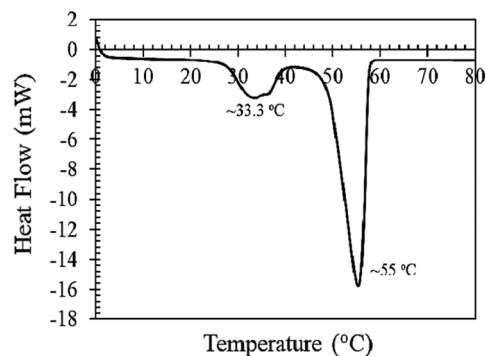


Figure 6: Differential scanning calorimeter plots showing the melting point of PCM III

For the case of PCM II, there were four endothermic peaks that were observed in the temperature range of 0°C to 55°C as illustrated in Fig. 5(a). The detail of the first endothermic peak is highlighted in Fig. 5(b). The first small endothermic peak was observed at approximately 7.4°C, which had a thermal absorption of 7.78 J/g. The second endothermic peak occurred around 25.9°C and had a thermal absorption of 20.02 J/g. This step could be the beginning of PCM II transitioning from a solid into a liquid. A third small endothermic

peak with a latent heat of 2.71 J/g and the last broad endothermic peak with an involved enthalpy of 147.79 J/g appeared around 31.6°C and 50.0°C, respectively. The paraffin continually absorbed thermal energy from the first to the third endothermic peaks as the PCM II changed phase from the solid state to the liquid state.

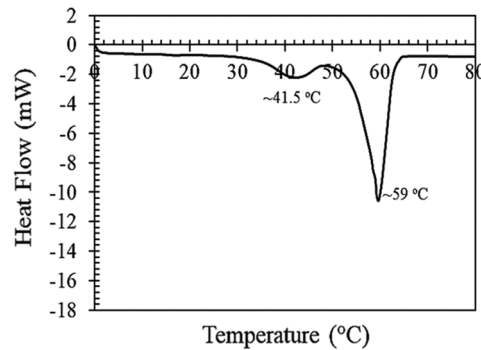


Figure 7: Differential scanning calorimeter plots showing the melting point of PCM IV

The endothermic peaks of PCM III in the temperature range of 0°C to 80°C are shown in Fig. 6. There are two endothermic peaks: The first endothermic peak was observed at approximately 33.3°C with a related enthalpy of 34.37 J/g. This step relates to some of the PCM III becoming molten. Another broad endothermic peak was observed at approximately 55.0°C with an enthalpy of 153.32 J/g, which corresponds to the PCM III melting from the solid to liquid state and this peak is continuous with the first endothermic peak. DSC thermal analysis of PCMIV is shown in Fig. 7. Two endothermic peaks were clearly present around 41.5°C with an enthalpy of 22.13 J/g for the first endothermic peak and 59.0°C, with an enthalpy of 137.67 J/g, for the second broad endothermic peak. These peaks represent the energy absorbed as the PCM IV melted from a solid to a liquid. These results demonstrated that the different paraffins have the ability to store thermal energy and the range of the temperatures during the phase transition of PCM I, PCM II, PCM III and PCM IV are appropriate to study the thermal behavior of phase change materials integrating into sheet metal roofing.

3.2 Thermal Behavior of Sheet Metal Roofing Integrated with Phase Change Materials

3.2.1 Temperature Variations at Each Location for Different Roof Models

While controlling the exterior metal roof surface temperature (T_{OR}) of approximately 50°C, the exterior roofing sheet surface temperature (T_{OR}), the space temperature over the metal roofing sheet (T_{AR}), interior metal roofing sheet surface temperature (T_{IR}), space temperature of the attic (T_{AA}), exterior ceiling surface temperature (T_{UC}), inside room temperature (T_R) and ambient temperature (T_A) were measured and recorded for 360 minutes to observe the temperature variation in each condition, as shown in Fig. 8 and Tab. 1. Fig. 8(a) shows the temperature in each position of the normal sheet metal roof (no-PCM). The exterior metal roof surface temperature (T_{OR}) was controlled independent of the surrounding temperature, at a temperature of approximately 50°C. The temperature at each position of the normal sheet metal roof (no-PCM) increased and then became stable after 40 min. The average temperatures after 40 min were calculated for each location and are exhibited in Tab. 1. The average temperatures at the positions of above the metal roofing sheet (T_{AR}), interior metal roof surface (T_{IR}), space temperature of the attic (T_{AA}), exterior ceiling surface (T_{UC}) and ambient (T_A) were around 47.4°C, 44.1°C, 30.2°C, 29.8°C and 27.0°C, respectively. It was observed that the average temperatures just above the metal roofing sheet (T_{AR}) is lower than the exterior metal roof surface temperature (T_{OR}). This implies the temperature of the exterior roof surface, measured by the thermocouples, is mainly affected by absorbing thermal radiation from the heat source lamps. The temperature trend of the metal roof sheet integrating PCM I, PCM II, PCM III

and PCM IV in each position was similar to that of the normal sheet metal roof as illustrated in Figs. 8(b)–8(e). The average temperatures in each position of the metal roof sheet integrating PCM I, PCM II, PCM III and PCM IV are exhibited in Tab. 1. When the temperature of the exterior roof surface was increased from 50°C to 80°C, an increase in the average temperatures for each position for all models was observed as shown in Tab. 1.

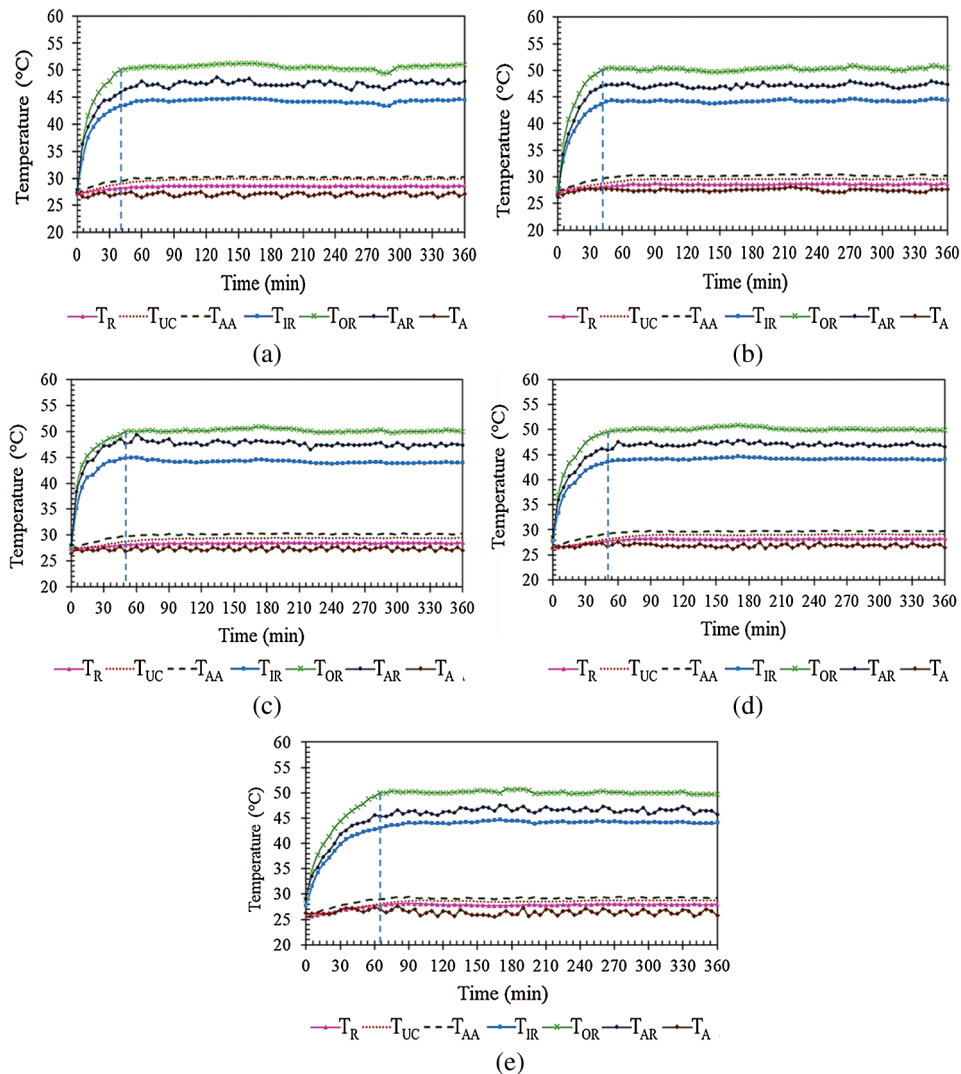


Figure 8: Temperature variations of metal sheet roof incorporating the PCM layer. (a) No-PCM, (b) PCM I, (c) PCM II, (d) PCM III and (e) PCM IV at the controlled temperature of 50°C

However, the integration of PCM I, PCM II, PCM III or PCM IV into the metal roof sheet affected the amount of time needed before a stable temperature was reached as a result of the different thermo-physical properties of PCM I, PCM II, PCM III and PCM IV as described in Section 3.1. The time to reach a steady temperature for each condition was further investigated and analyzed. When the exterior roof surface temperature was held at approximately 50°C, the temperature at each position for the various PCMs was observed to measure the time before a steady temperature was reached. The time it took to absorb enough thermal energy to reach a stable temperature increased from 40 min to 65 min when the metal roof sheet integrated PCMs which were sequentially exchanged in the order of: PCM I, PCM II, PCM III and

PCM IV-layer, as displayed in Fig. 9. The longest time to absorb enough thermal energy before reaching a steady temperature was found for the roof that integrated PCM IV into the metal roof sheet, and was approximately 65 min. The time delay before reaching steady temperature in this model was higher than the normal model (without the PCM layer) and the models integrating PCM I, PCM II or a PCM III layer by around 62.5%, 62.5%, 30.0%, and 8.3%, respectively.

Table 1: Average temperature at the positions of: the space above metal roofing sheet (T_{AR}), inside surface of the metal sheet (T_{IR}), inner space of the attic (T_{AA}), upper ceiling surface temperature (T_{UC}) and ambient space (T_A) under the different controlled conditions

		Average temperature at each position (°C)				
		T_{AR}	T_{IR}	T_{AA}	T_{UC}	T_A
$T_{con} = 50^{\circ}C$ (T_{OR})	no-PCM	47.4	44.1	30.2	29.8	27.0
	PCM I	47.4	44.1	30.1	29.6	27.1
	PCM II	47.5	44.2	30.0	29.4	27.0
	PCM III	47.5	44.2	29.7	29.0	26.9
	PCM IV	47.6	44.3	29.3	28.7	27.0
$T_{con} = 60^{\circ}C$ (T_{OR})	no-PCM	55.2	51.1	31.2	30.4	27.1
	PCM I	55.2	51.1	31.0	30.1	27.1
	PCM II	55.3	51.1	31.0	30.1	27.0
	PCM III	55.5	51.3	30.8	30.0	27.2
	PCM IV	55.5	51.3	30.7	29.8	27.0
$T_{cont} = 70^{\circ}C$ (T_{OR})	no-PCM	63.2	57.9	32.7	31.2	27.0
	PCM I	63.4	58.2	32.4	30.9	27.1
	PCM II	63.4	58.2	32.3	30.7	27.0
	PCM III	63.6	58.3	32.2	30.8	27.2
	PCM IV	63.9	58.5	32.3	30.8	27.0
$T_{con} = 80^{\circ}C$ (T_{OR})	no-PCM	73.4	65.9	33.6	32.2	27.0
	PCM I	73.6	66.0	32.6	31.9	27.0
	PCM II	73.6	66.0	32.5	31.6	27.2
	PCM III	73.9	66.2	32.5	31.5	27.1
	PCM IV	74.2	66.3	32.4	31.4	27.0

The normal sheet metal roof (without a PCM layer) reached steady values around 40 min at $50^{\circ}C$ and 60 min at $80^{\circ}C$. This tendency of increasing time to reach steady state from absorbing thermal energy of the sheet metal roofs integrating PCM I, PCM II, PCM III and PCM IV, is similar to that of the normal metal roof sheet as shown in Fig. 9. The metal roof sheet integrating PCM IV could significantly extend the times before reaching steady temperature, by about 30 min, by absorbing thermal energy when compared with the normal model (without the PCM layer) in each temperature condition, as shown in Fig. 9. This causes a delay in heat transmission from the exterior roof surface into the interior testing room. Using phase change materials integrated into the sheet metal roofing reduced the heat transfer and interior room temperature which can provide energy saving for buildings. This is an important result.

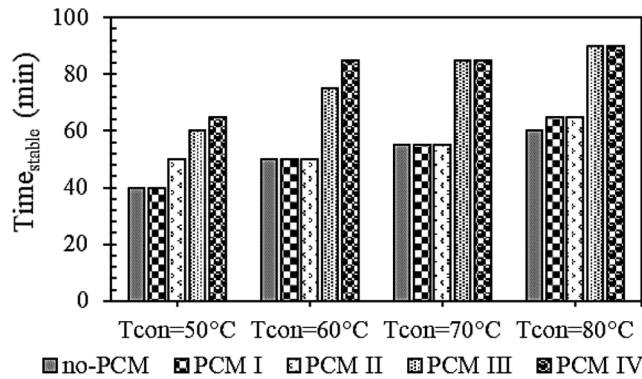


Figure 9: Time before stable temperature readings of roofing integrated with PCMs layer

3.2.2 Temperature Decrement Factor

The temperature decrement factors for both the exterior roof surface and interior space of the models with standard sheet metal and sheet metal sheet with integrated PCM I, PCM II, PCM III and PCM IV for the controlled temperatures of 50°C, 60°C, 70°C and 80°C are listed in Tab. 2. The temperature decrement factor (Φ) showed decrease in heat transmission through the exterior roof surface into the interior testing room for each condition. The temperature decrement factor was determined by the following Eq. (1).

$$\Phi = \frac{T_{OR} - T_R}{T_{OR}} \times 100\% \tag{1}$$

where T_{OR} is the exterior roofing sheet surface temperature and T_R is the inside temperature of the model. When considering the normal metal sheet roof, without a PCM layer, the average room temperature increased from 42.6% to 62.6% when the controlled exterior roof surface temperature increased from 50°C to 80°C. The tendency of the temperature decrement factor of the metal roof sheet integrating PCM I, PCM II, PCM III and PCM IV were similar to those of the normal metal roof sheet as demonstrated in Tab. 2.

Table 2: Temperature decrement factor through the outside roof surface into the inner space of the test room in each condition

	Percentage of temperature decrement factor (%)			
	T _{con} = 50°C	T _{con} = 60°C	T _{con} = 70°C	T _{con} = 80°C
no-PCM	42.6	51.7	57.9	62.6
PCM I	43.0	51.8	57.9	62.6
PCM II	43.6	52.0	58.1	62.8
PCM III	43.6	52.2	58.3	62.9
PCM IV	44.2	52.3	58.3	62.9

The temperature decrement factors for the roof of the reference model and models using the PCM I, PCM II, PCM III and PCM IV layers were approximately 42.6%, 43.0%, 43.6%, 43.6% and 44.2% under the controlled temperature of 50°C, approximately 51.7%, 51.8%, 52.0%, 52.2% and 52.3% under the controlled temperature of 60°C, approximately 57.9%, 57.9%, 58.1%, 58.3% and 58.3% under the controlled temperature of 70°C, and around 62.6%, 62.6%, 62.8%, 62.9% and 62.9% under the

controlled temperature of 80°C, respectively. For each controlled temperature, the maximum temperature decrement factors were found with the model integrating PCMIV into the sheet metal roof, and the values increased to around 3.7%, 1.2%, 0.7% and 0.5% when compared with that of the reference model under the controlled temperatures of 50°C, 60°C, 70°C and 80°C, respectively, as shown in Tab. 2. The increase in the temperature decrement factors for each controlled temperature was determined by the following Eq. (2).

$$\% \text{ increment of temperature decrement factor} = \left| \frac{\Phi_{\text{PCM}} - \Phi_{\text{without PCM}}}{\Phi_{\text{without PCM}}} \right| \times 100\% \quad (2)$$

where Φ_{PCM} is the percentage of the temperature decrement factor for the model integrating a layer of different PCM types and $\Phi_{\text{without PCM}}$ is the percentage of temperature decrement factor for the model without a PCM layer. The integration of PCM IV into the metal sheet roof demonstrated a minor increase in the temperature decrement factor, which relates to a decline in the heat transmission through the exterior roof surface into the inside space of the testing room and which can result in energy savings for buildings and can significantly reduce the peak cooling requirement.

3.2.3 Average Inside Room Temperature

Fig. 10 displays the average room temperatures for the models with and without integrating PCM I, PCM II, PCM III, or a PCM IV layer in each condition for the different controlled temperatures. For the situation where the exterior roof surface temperature was held at 50°C, a decline in the average room temperature for each model was achieved when PCM I, PCM II, PCM III or a PCM IV layer was integrated into the metal roof sheet. The average room temperature of the reference model and models using PCM I, PCM II, PCM III or PCM IV layer were around 28.7°C, 28.5°C, 28.2°C, 28.2°C and 27.9°C, respectively. The percentage the average room temperatures decreased for the testing model integrating the PCM I, PCM II, PCM III or PCM IV layer was approximately 0.7%, 1.7%, 1.7% and 2.8% when compared with that of the model without PCM under a controlled temperature of 50°C, which were calculated by the following Eq. (3).

$$\% \text{ lower room temperature} = \left| \frac{T_{\text{R(PCM)}} - T_{\text{R(without PCM)}}}{T_{\text{R(without PCM)}}} \right| \times 100\% \quad (3)$$

where $T_{\text{R(PCM)}}$ is the room temperature of the model integrating PCM I, PCM II, PCM III, or a PCM IV layer and $T_{\text{R(without PCM)}}$ is the room temperature of the model without a PCM layer. For each condition with a different controlled temperature, the trend of the interior temperature for the reference model and the models integrating PCM I, PCM II, PCM III and PCM IV were similar to the trends for the controlled temperature of 50°C, as exhibited in Fig. 10.

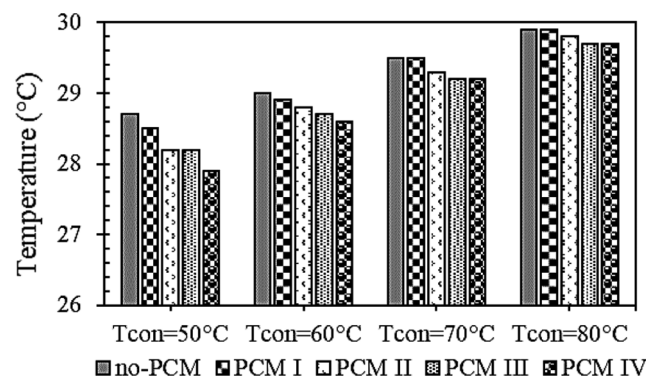


Figure 10: Average room temperature for each temperature condition

In the case of the reference model (without a PCM layer), the average room temperature increased from 28.7°C to 29.9°C when the exterior roof surface temperature increased from 50°C to 80°C. The trend of the average room temperature for the metal roof sheets integrating PCM I, PCM II, PCM III or PCM IV as similar to the normal metal roof sheet as exhibited in Fig. 10. For each temperature, the metal roof sheet integrating PCM IV can best reduce the average room temperature, which was caused by the reduced heat transmission through the exterior roof surface into the interior testing room. However, a numerical simulation based on these experimental results could lead to a more sound scientific knowledge, but has not been performed at this time. Therefore, this will be analyzed and investigated in future work. In view of the benefits, using a phase change materials integrated into the metal roof sheet could also provide a significant reduction in the energy requirement of buildings and reduce the yearly peak cooling demand.

4 Conclusions

The integration of phase change materials into a metal roofing sheet was studied by utilizing PCMs with different melting points for different conditions, to study the effects of PCMs on the thermal performance of a roof. Lower room temperatures for the sheet metal roof integrating phase change materials with melting points around 45°C, 50°C, 55°C or 59°C were obtained, which reduced the room temperature up to 0.7%, 1.7%, 1.7% and 2.8% when the outer roof surface temperature was controlled at 50°C, compared to the reference sheet metal roof. The time until a steady temperature was reached increased for the model integrating PCM IV layer by approximately 62.5%, 62.5%, 30.0%, and 8.3%, respectively, when compared to the reference model, the model integrating PCM I, PCM II or a PCM III layer. Moreover, the model integrating PCM IV can increase the temperature decrement factor value around 3.7%, 1.2%, 0.7% and 0.5% when compared with that of the reference model under the controlled temperatures of 50°C, 60°C, 70°C and 80°C. The integration of phase change materials into sheet metal roofing of buildings could lead to lower room temperatures and a larger temperature gradient, by enhancing the insulating properties of the metal roof. This would lead to a reduction in energy consumption from the cooling load of air conditioners and a decline in yearly peak cooling demand.

Acknowledgement: Thanks are given to Dr. Kyle V. Lopin for editing this document.

Funding Statement: The authors would like to thank the Thailand Science Research and Innovation (TSRI), Faculty of Science, Naresuan University for providing financial support to this research work, and our research center.

Conflicts of Interest: The authors declare that they have no conflicts of interest to report regarding the present study.

References

1. Guan, X., Wei, H., Lu, S., Dai, Q., Su, H. (2018). Assessment on the urbanization strategy in China: Achievements, challenges and reflections. *Habitat International*, 71, 97–109. DOI 10.1016/j.habitatint.2017.11.009.
2. Avtar, R., Tripathi, S., Aggarwal, A. K., Kumar, P. (2019). Population–urbanization–energy nexus: A review. *Resources*, 8(3), 136. DOI 10.3390/resources8030136.
3. Kim, B., Neff, R. (2009). Measurement and communication of greenhouse gas emissions from U.S. food consumption via carbon calculators. *Ecological Economics*, 69(1), 186–196. DOI 10.1016/j.ecolecon.2009.08.017.
4. Barzin, R., Chen, J. J., Young, B. R., Farid, M. M. (2015). Application of PCM energy storage in combination with night ventilation for space cooling. *Applied Energy*, 158, 412–421. DOI 10.1016/j.apenergy.2015.08.088.
5. Shaikh, P. H., Nor, M. N. B., Nallagownden, P., Elamvazuthi, I., Ibrahim, T. (2014). A review on optimized control systems for building energy and comfort management of smart sustainable buildings. *Renewable and Sustainable Energy Reviews*, 34, 409–429. DOI 10.1016/j.rser.2014.03.027.

6. Catrini, P., Panno, D., Cardona, F., Piacentino, A. (2020). Characterization of cooling loads in the wine industry and novel seasonal indicator for reliable assessment of energy saving through retrofit of chillers. *Applied Energy*, 266, 114856. DOI 10.1016/j.apenergy.2020.114856.
7. Marin, P., Saffari, M., De Gracia, A., Zhu, X., Farid, M. M. et al. (2016). Energy savings due to the use of PCM for relocatable lightweight buildings passive heating and cooling in different weather conditions. *Energy and Buildings*, 129, 274–283. DOI 10.1016/j.enbuild.2016.08.007.
8. Akeiber, H., Nejat, P., Majid, M. Z. A., Wahid, M. A., Jomehzadeh, F. et al. (2016). A review on phase change material (PCM) for sustainable passive cooling in building envelopes. *Renewable and Sustainable Energy Reviews*, 60, 1470–1497. DOI 10.1016/j.rser.2016.03.036.
9. Chang, P. C., Chiang, C. M., Lai, C. M. (2008). Development and preliminary evaluation of double roof prototypes incorporating RBS (radiant barrier system). *Energy and Buildings*, 40(2), 140–147. DOI 10.1016/j.enbuild.2007.01.021.
10. Yew, M. C., Yew, M. K., Saw, L. H., Nga, T. C. Chen, K. P. et al. (2018). Experimental analysis on the active and passive cool roof systems for industrial buildings in Malaysia. *Journal of Building Engineering*, 19, 134–141. DOI 10.1016/j.jobee.2018.05.001.
11. Fernandes, D., Pitié, F., Cáceres, G., Baeyens, J. (2012). Thermal energy storage: How previous findings determine current research priorities. *Energy*, 39(1), 246–257. DOI 10.1016/j.energy.2012.01.024.
12. Balaras, C. A. (1996). The role of thermal mass on the cooling load of buildings. An overview of computational methods. *Energy and Buildings*, 24(1), 1–10. DOI 10.1016/0378-7788(95)00956-6.
13. Alva, G., Lin, Y., Liu, L., Fang, G. (2017). Synthesis, characterization and applications of microencapsulated phase change materials in thermal energy storage: A review. *Energy and Buildings*, 144, 276–294. DOI 10.1016/j.enbuild.2017.03.063.
14. Liang, F., Zhang, Y., Liu, Q., Jin, Z., Zhao, X. et al. (2017). Experimental study on thermal energy storage performance of water tank with phase change materials in solar heating system. *Procedia Engineering*, 205, 3027–3034. DOI 10.1016/j.proeng.2017.10.257.
15. Chiew, J., Chin, C. S., Jia, J., Toh, W. D., Gao, Z. (2017). Effects of void spaces in a phase change material based thermal energy storage system. *Energy Procedia*, 143, 559–565. DOI 10.1016/j.egypro.2017.12.727.
16. Alqallaf, H. J., Alawadhi, E. M. (2013). Concrete roof with cylindrical holes containing PCM to reduce the heat gain. *Energy and Buildings*, 61, 73–80. DOI 10.1016/j.enbuild.2013.01.041.
17. Alawadhi, E. M., Alqallaf, H. J. (2011). Building roof with conical holes containing PCM to reduce the cooling load: Numerical study. *Energy Conversion and Management*, 52(8–9), 2958–2964. DOI 10.1016/j.enconman.2011.04.004.
18. Meng, E., Wang, J., Yu, H., Cai, R., Chen, Y. et al. (2019). Experimental study of the thermal protection performance of the high reflectivity-phase change material (PCM) roof in summer. *Building and Environment*, 164, 106381. DOI 10.1016/j.buildenv.2019.106381.
19. Kośny, J., Biswas, K., Miller, W., Kriner, S. (2012). Field thermal performance of naturally ventilated solar roof with PCM heat sink. *Solar Energy*, 86(9), 2504–2514. DOI 10.1016/j.solener.2012.05.020.
20. Chou, H. M., Chen, C. R., Lan, N. V. (2013). A new design of metal-sheet cool roof using PCM. *Energy and Buildings*, 57, 42–50. DOI 10.1016/j.enbuild.2012.10.030.
21. Thongtha, A., Boontham, P. (2020). Experimental investigation of natural lighting systems using cylindrical glass for energy saving in buildings. *Energies*, 13(10), 2528. DOI 10.3390/en13102528.
22. Thongtha, A., Khongthon, A., Boontham, P., Chan, H. Y. (2019). Thermal effectiveness enhancement of autoclaved aerated concrete wall with PCM-contained conical holes to reduce the cooling load. *Materials*, 12(13), 2170. DOI 10.3390/ma12132170.
23. Bengtsson, L. P., Whitaker, J. H. (1986). *Farm structures in tropical climates: A textbook for structural engineering and design*. Rome: FAO, Italy.